Dissimilar Resistance Spot Welding of Aluminum to Magnesium with Zn-Coated Steel Interlayers

High-strength dissimilar Al/Mg joints can be produced by resistance spot welding with an interlayer

BY P. PENNER, L. LIU, A. GERLICH, AND Y. ZHOU

ABSTRACT

Resistance spot welding of AZ31B Mg alloy to Al Alloy 5754 was studied using Zn foil and Zn-coated steel interlayers. Mechanical properties and microstructure of the welds were analyzed. The strength requirements of AWS Standard D17.2 could not be met when a Zn foil interlayer was used. However, acceptable joint strengths were achieved using a Zn-coated steel interlayer, since the steel remains solid and can successfully keep Al and Mg from mixing. An ultrathin Fe-Al layer present at the Zn-coating interface of the steel interlayer promoted metallurgical bonding at both Al and Mg alloy interfaces. Welds made with Zn-coated steel interlayers met the strength requirements of the AWS standard and reached 74% of the strength of comparable AZ31B similar resistance spot welds.

KEYWORDS

Magnesium • Aluminum • Zinc • Steel • Dissimilar • Resistance Spot Welding • Interlayer

Introduction

To improve fuel efficiency, aerospace and automotive industries have strived for component weight reduction. One of the common approaches to reducing the weight of structural components is the use of light Al and Mg alloys. Resistance spot welding (RSW) is commonly used in both automotive and aerospace industries. With the increased use of Al and Mg, there is a pressing need for a technology to produce dissimilar Al/Mg joints, preferably with RSW since this technology is already prevalent in those industries. Direct welding of Al to Mg usually results in formation of hard and brittle intermetallic compounds and poor quality welds (Refs. 1–3). Employing an interlayer is a promising approach to overcoming this problem. Numerous studies investigating Al/Mg joints made with different interlayers such as Zn (Refs. 4–8), Ni (Refs. 9, 10), Ce (Ref. 11), Ti (Ref. 12), and others (Refs. 13–15) can be found in the literature. Most of the studies reported that employing an interlayer reduced the amount of brittle Al-Mg compounds and improved mechanical properties of the joints. At the moment, Zn is the most studied interlayer for Al/Mg joining. All the studies that employed a Zn interlayer reported the addition of Zn greatly improved weld strength, especially when Al and Mg were completely separated (Ref. 8). Besides Zn foil, the use of a Au-coated Ni interlayer has also been studied in detail (Ref. 16). Though this study showed some promising results, there is still a need for alternative interlayers with lower cost and better availability. Another strong candidate for the interlayer for Al/Mg RSW is hot-dip galvanized Zn-coated steel. Recent studies on joining of Mg to galvanized steels reported Mg can be successfully joined to galvanized steels by RSW (Refs. 17, 18), due to the presence of an ultrathin Fe-Al intermetallic layer that always forms between the Zn coating and steel during the galvanizing process (Refs. 19, 20). Literature also indicates that Al can be easily spot welded to steel due to formation of a continuous Fe-Al reaction layer during welding (Refs. 21–23). Therefore, it is of interest to study dissimilar RSW of Al to Mg with Zn-foil and Zn-coated steel interlayers.

Experimental

Welding specimens used in this study were sheets of Mg alloy AZ31B-H24 and Al Alloy 5754-O, with nominal ultimate tensile strengths of 285 and 215 MPa,

*P. PENNER (ppenner@uwaterloo.ca) is with Centre for Advanced Materials Joining, University of Waterloo, Waterloo, Canada. A. GERLICH (*agerlich@uwaterloo.ca*) is an associate professor, and Y. ZHOU (*nzhou@uwaterloo.ca*) is a professor, Centre for Advanced Materials Joining, University of Waterloo, Waterloo, Canada. L. LIU (*ray.plasma@gmail.com*) is with Department of Mechanical Engineering, Tsinghua University, Beijing, China.*

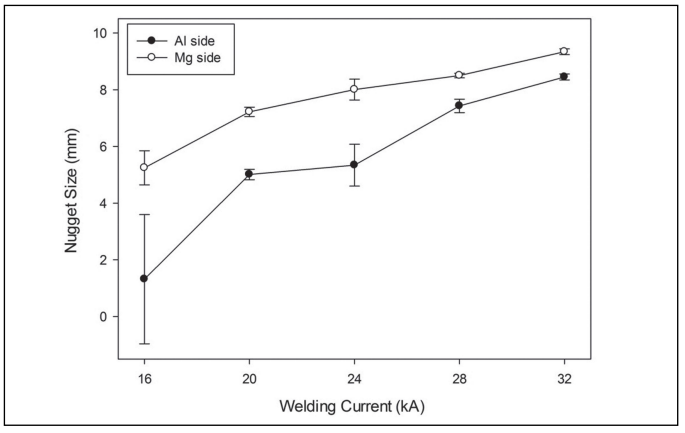

Fig. 1 — Correlation between nugget size on Al and Mg sides and welding current during RSW with a Zn-coated steel interlayer.

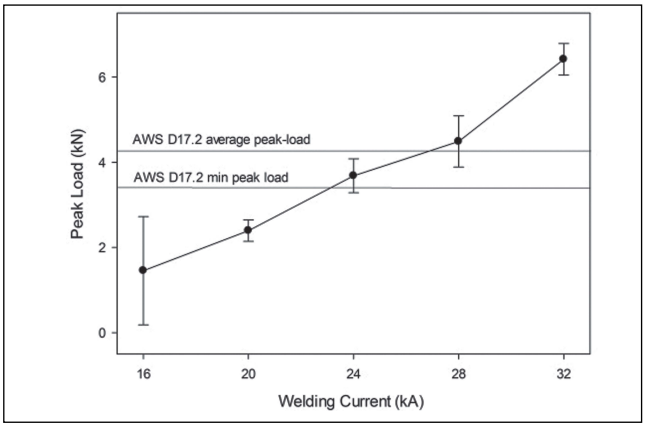

Fig. 2 — Correlation between peak load and welding current during RSW of Al to Mg with Zn-coated steel interlayer.

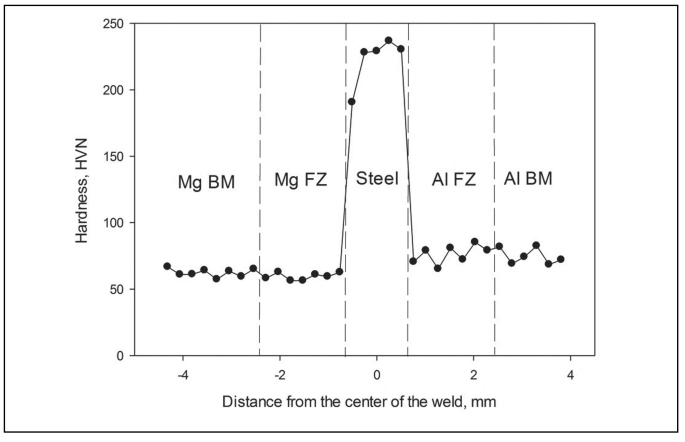

Fig. 3 — Hardness distribution across Al/Mg weld made with a Zn-coated steel interlayer and 28-kA welding current.

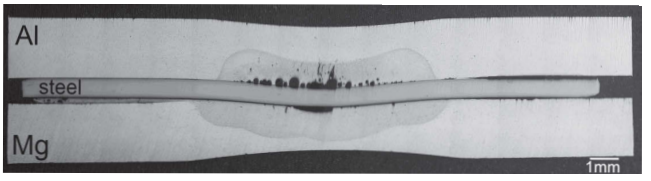

Fig. 4 — Typical Al/Mg weld made with a Zn-coated steel interlayer and 28-kA welding current.

respectively (Refs. 24, 25). Dimensions of the Al and Mg alloy welding coupons were 100 × 35 × 2 mm. Commercially pure Zn foil with thickness of 0.25 mm and hot-dip galvanized HSLA steel with thickness of 0.7 mm were used as interlayers in this study. Interlayers of both types were 20 × 20 mm in size. In our previous study (Ref. 26), Zn/steel interface of the steel interlayer used in this study was examined and it was found that there is an increase in Al content between the Zn coating and the steel. This confirms the presence of a nanoscale layer of Fe-Al intermetallic in the galvanized steel used in this study. The thickness of the Zn coating was 10 μm on both sides of the steel sheet.

A MFDC resistance spot welding machine was used in the current study with the following parameters: welding current in a range of 16–32 kA, 5 cycles welding time, and 4-kN electrode force. Type FF25 electrode caps were used and had a spherical radius of 50.8 mm and a face diameter of 16 mm, manufactured from Cu-Cr-Zr alloy. After welding at least three coupons for each welding condition, they were tested on an Instron tensile shear test machine. Metallographic weld coupons and the fracture surface of the samples were analyzed using optical and scanning electron microscopy (SEM). Nugget sizes of welds were measured from cross sections, with three measurements for each welding condition. Vickers microhardness test was performed along the diagonal across the weld. Each indentation was made with a 100-g load and 15-s indentation time, with the distance between each indentation equal to 0.25 mm.

Results and Discussion

Mechanical Properties

The use of a 0.25-mm-thick pure Zn foil interlayer was first attempted with welding currents of 16 to 32 kA. Joint strengths could not meet the requirements of AWS D17.2, *Specification of Resistance Welding for Aerospace Applications*, and it is likely that extensive intermetallic formation occurred in the nugget. This was evidenced by microhardness values of 224 to 304 HV in the nugget zone. Since poor quality welds were produced with a Zn-foil interlayer due to mixing of Al, Mg, and Zn, a Zn-coated steel interlayer was considered instead to prevent the mixing of the molten Al and Mg alloys.

Figure 1 shows the relationship between nugget size and welding current for welds made with the Zn-coated steel interlayer. It was noted that the nugget on the Mg side always was larger than that on the Al side. The same observation was made in our previous study, which investigated effects of Ni-based interlayers on Al/Mg resistance spot welds (Ref. 16). Al 5754 alloy has lower electrical resistivity and higher thermal conductivity (49 nΩm and 147 W m^{-1} K^{-1}, respectively)(Ref. 25) compared to AZ31B Mg alloy (92 nΩm and 96 W m^{-1} K^{-1}, respectively) (Ref. 25), which would lead to lower heat generation and greater heat losses on the Al side. Therefore, smaller nugget size should

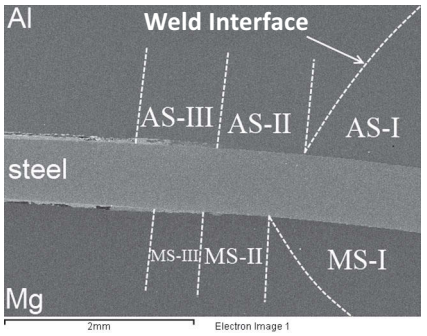

Fig. 5 — Location of the zones that exhibit different interfacial microstructures in an Al/Mg weld made with a Zn-coated steel interlayer and 28-kA welding current.

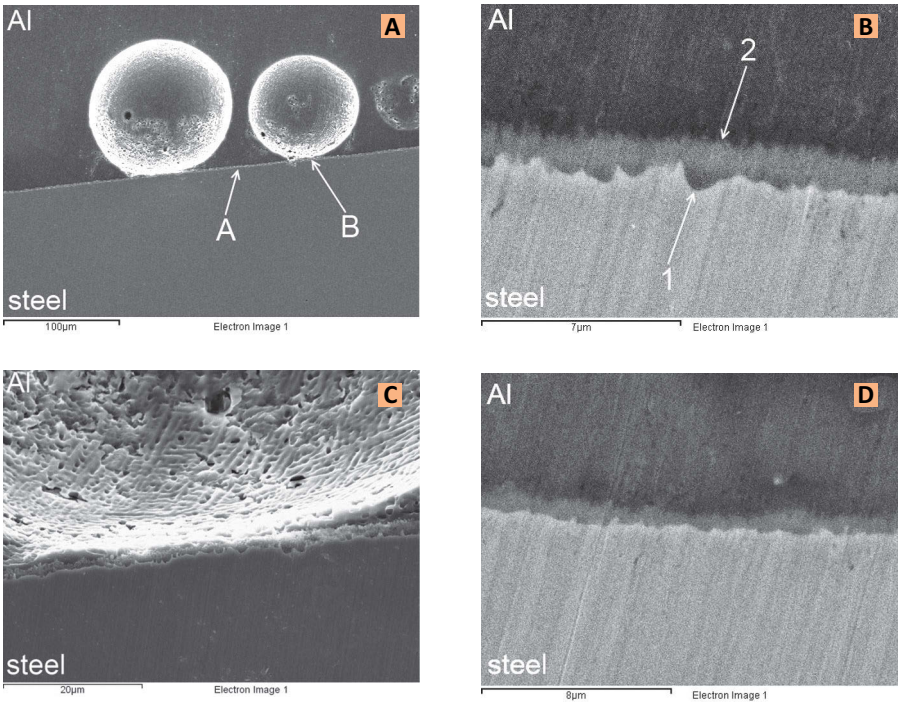

Fig. 6 — Al/steel interface of zone AS-I from Fig. 5: A — Center of AS-I; B — details of A from A; C — details of B from A; D — zone AS-I close to the boundary with AS-II.

be expected at the Al side of the weld.

During tensile shear testing, samples made with all welding currents failed at the Al/steel interface, suggesting that the Mg/steel interface was stronger. As shown in Fig. 2, welds made with a welding current of 28 kA and higher easily met the strength requirements of AWS D17.2. The average peak load reached 74% of the comparable AZ31B similar joints (Refs. 27, 28). Welding currents >32 kA were not investigated since these would likely begin to promote expulsion.

Figure 3 shows hardness distribution across a typical Al/Mg weld made with a Zn-coated steel interlayer. It can be observed that hardening did not occur either in the Mg or Al alloy fusion zones, which suggests that formation of a large amount of brittle intermetallics was avoided. This was expected since the steel interlayer remained solid and separated the Al and Mg from mixing and intermetallic formation, and also suggests that negligible intermetallics were formed involving Zn due to the low quantity of this element originating from the coating.

Interfacial Microstructure and Fracture Morphology

Al/Steel Interface

Interfacial Microstructure

Figure 4 shows an optical micrograph of a typical Al/Mg weld made with a Zn-coated steel interlayer. There were much more interfacial defects such as voids at the Al/steel interface than at the Mg/steel interface, which is believed to contribute to weld fracture at the Al/steel interface.

There are three distinct zones in the Al/steel interface such as shown in Fig. 5. The interface inside the fusion nugget was denoted as AS-I, the region adjacent to the nugget as AS-II, and the region where welding occurred through the Zn-rich phase, as zone AS-III.

Details of the Al/steel interface at zone AS-I are shown in Fig. 6 (Table 1). Figure 6A–C shows the center of a nugget while Fig. 6D shows the edge of zone AS-I (edge of the fusion zone). None of the Zn coating can be found between the Al and steel anywhere in zone AS-I. Zinc was melted and squeezed from the nugget due to its low melting point (420°C) (Ref. 24).

Microstructures of the interface at the center of the nugget (Fig. 6B) exhibit a distinct Al-Fe reaction layer with an average thickness of 1.3 µm. From Fig. 6C, it can be seen that voids were located close to the Al-Fe reaction layer. Almost no voids were observed at the edge of the nugget, while the Al-Fe reaction layer still was present.

Table 1 — Energy-Dispersive X-Ray Analysis Quantification of Different Areas in Fig. 6 (wt-%)

Spectrum	Al	Fe	Mg	Zn
1	42.4	57.6	—	—
2	60.6	36.0	3.4	—

However, the average thickness of the reaction layer at the edge of the fusion nugget was 0.65 µm, which is half of that in the center. Qiu et al. (Refs. 21–23) also found that in dissimilar RSW of Al to steel, the thickness of the Al-Fe reaction layer decreases from the center to the edge of a nugget, and they explained this by the fact that more heat usually generates at the center of a resistance spot weld, which results in formation of a thicker reaction layer in the center. This also likely accounts for the variation in the reaction layer thickness observed in the current study. It is obvious that the Fe-Al reaction layer at the Al/steel interface formed due to the reaction between molten Al and steel surface during the welding, since the ultrathin Fe-Al layer prefabricated between Zn-coating and steel before welding was much thinner than 0.65 µm. Overall, a

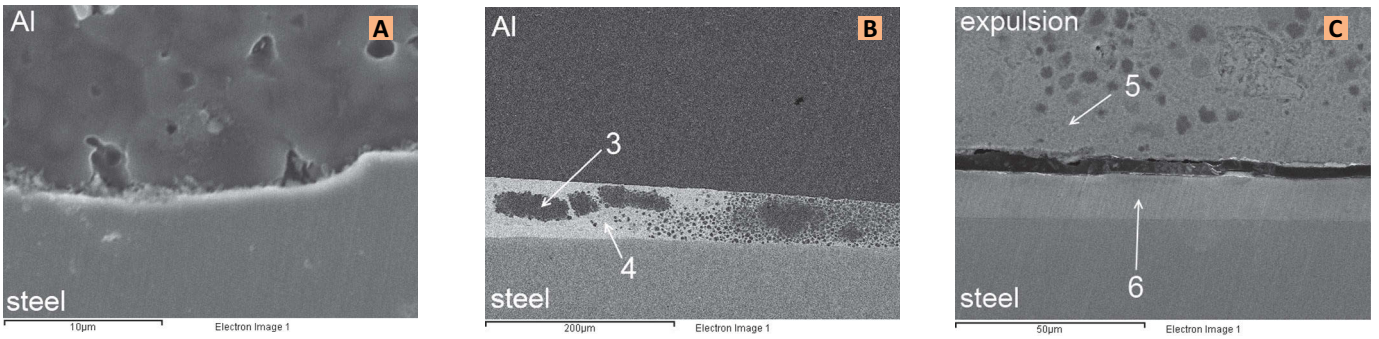

Fig. 7 — Al/steel interface beyond the fusion nugget, which corresponds to interfaces noted in Fig. 5. A — Zone AS-II; B — zone AS-III; C — region beyond AS-III.

Table 2 — Energy-Dispersive X-Ray Analysis Quantification of Different Areas in Fig. 7 (wt-%)

Spectrum	Al	Zn
3	100	—
4	25.5	74.5
5	25.8	74.3
6	—	100

reaction layer observed at the Al/steel interface (Fig. 6) should not severely deteriorate the strength of the joints since cracks were not observed, and the maximum thickness of intermetallics did not exceed 1.3 mm. It was reported by Qiu et al. (Ref. 23) that only Al-Fe reaction layers thicker than 1.5 µm can negatively influence the strength.

Figure 7A shows the Al/steel interface at the region adjacent to the nugget (which was marked as AS-II in Fig. 5). Some discontinuous Al-Fe reaction products can also be observed at the interface. None of the Zn coating layer can be found at this region, suggesting that Zn was squeezed further to zone AS III and beyond.

Figure 7B shows the Al/steel interface at zone AS-III. It can be seen that a significant reaction occurred between the Zn coating and Al sheet in the region. The Zn-Al reaction layer in the region was approximately 50 mm thick, which is five times larger than the thickness of the original Zn coating. Zinc likely was squeezed from the fusion nugget (zone AS-I) toward the outer nugget region (zone AS-II) and to zone AS-III where it reacted with Al. Microstructure of the Zn-Al reaction layer suggests that it was formed by an interdiffusion process. Welding in the region occurred through this Zn-Al reaction product.

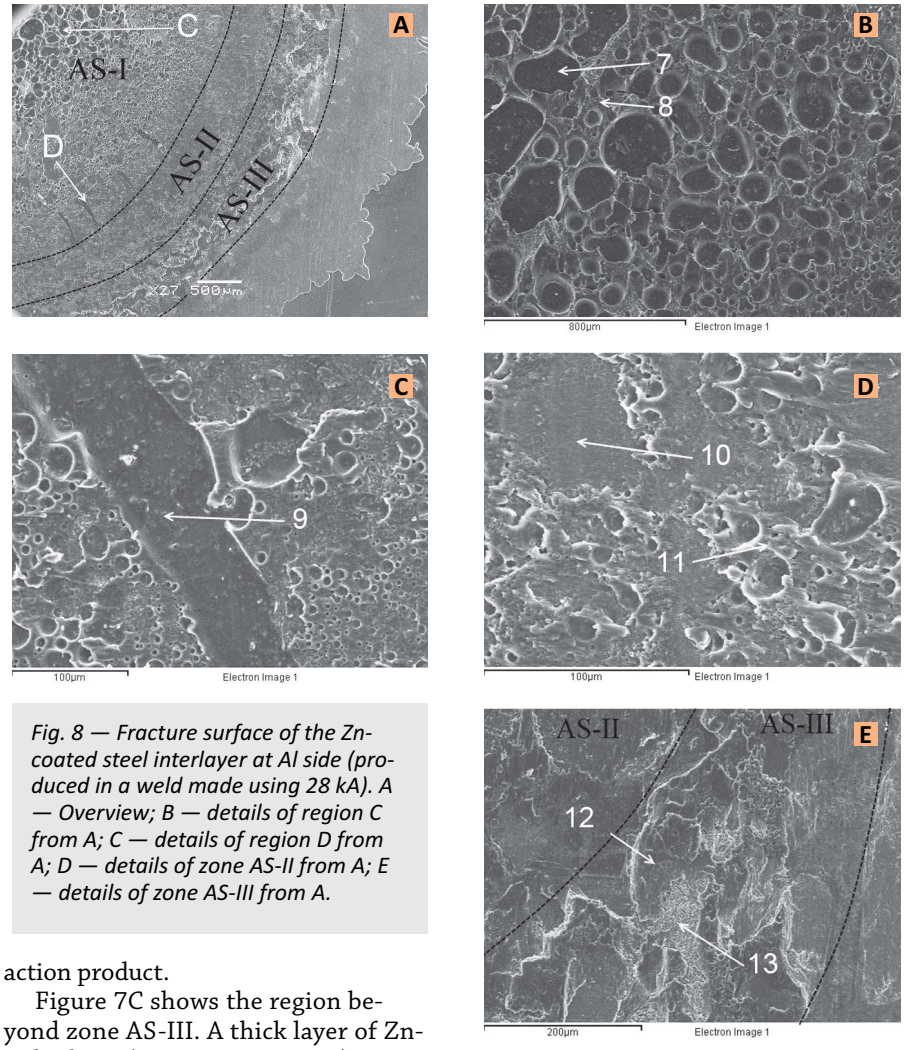

Fig. 8 — Fracture surface of the Zn-coated steel interlayer at Al side (produced in a weld made using 28 kA). A — Overview; B — details of region C from A; C — details of region D from A; D — details of zone AS-II from A; E — details of zone AS-III from A.

Figure 7C shows the region beyond zone AS-III. A thick layer of Zn-rich phase (region 5 in Fig. 7C) was observed as well as the intact original Zn coating (region 6 in Fig. 7C), which suggests that no welding occurred in the region. Overall, the interfacial microstructure of the Al/steel interface suggests that welding occurred between Al and steel in zones AS-I, AS-II, and AS-III marked on Fig. 5, while no welding occurred beyond zone AS-III. Zinc was melted and squeezed from the fusion nugget, leading to direct weld brazing in the fusion nugget area (AS-I), solid-state welding at the region adjacent to the nugget (AS-II), and soldering via the Zn-rich filler metal next to the solid-state welding region (Table 2).

Fracture Morphology

Figure 8 shows the fracture surface of the Zn-coated steel interlayer at the Al side. Regions of the fracture surface that correspond to the interfacial microstructure zones AS-I, AS-II, and AS-III (Fig. 5) are shown in Fig. 8A. It can be seen from Fig. 8B that in the center of zone AS-I failure occurred inside the Al fusion zone close to the interface since pores that concentrated near the interface can be observed on the fracture surface (region 7 in Fig. 8B). An Fe-Al intermetallic compound layer with a flat surface can be found under the voids, and ductile fracture surfaces corresponding to the Al alloy fusion zone can be found between the voids (region 8 in Fig. 8B), which suggests that porosity decreased joint strength. Figure 8C shows the edge of the AS-I zone (region D in Fig. 8A). The fracture morphology of this region is similar to that of the center of zone AS-I, but the size of the voids in this region is considerably smaller than in the center. A few river-like voids (region 9 in Fig. 8C) can be observed in the region. Usually river-like voids form as a result of accumulation of smaller voids (Ref. 29), and this appears to be the same phenomenon in the current study.

Figure 8D shows the fracture morphology of zone AS-II, which was adjacent to the fusion nugget, and appears to be where solid-state welding between Al and steel occurred — Fig. 7A. The surface morphology of the region suggests that fracture occurred either at the Al/steel interface (region 10 in Fig. 8D) or inside the Al sheet (region 11 in Fig. 8D). Figure 8E shows the fracture surface of zone AS-III where the Al-Zn reaction layer was observed at the Al/steel interface — Fig. 7B. The fracture morphology and chemical composition (Table 3) of the region suggest that failure occurred partially inside the Al sheet (region 12 in Fig. 8E) and partially inside the Al-Zn reaction layer (region 13 in Fig. 8E). Based on the fracture morphology and interfacial microstructure analysis (Fig. 7B), it can be concluded that welding in this region was promoted by the presence of Zn, which contributed to the strength.

Analysis of the fracture morphology confirmed the findings made during the interfacial microstructure analysis, in particular that zones AS-I, AS-II, and AS-III contributed to the strength and that joining occurred by direct weld brazing in the fusion nugget area, by solid-state welding in the zone adjacent to the nugget, and by brazing through the Zn filler metal next to the solid-state welding region.

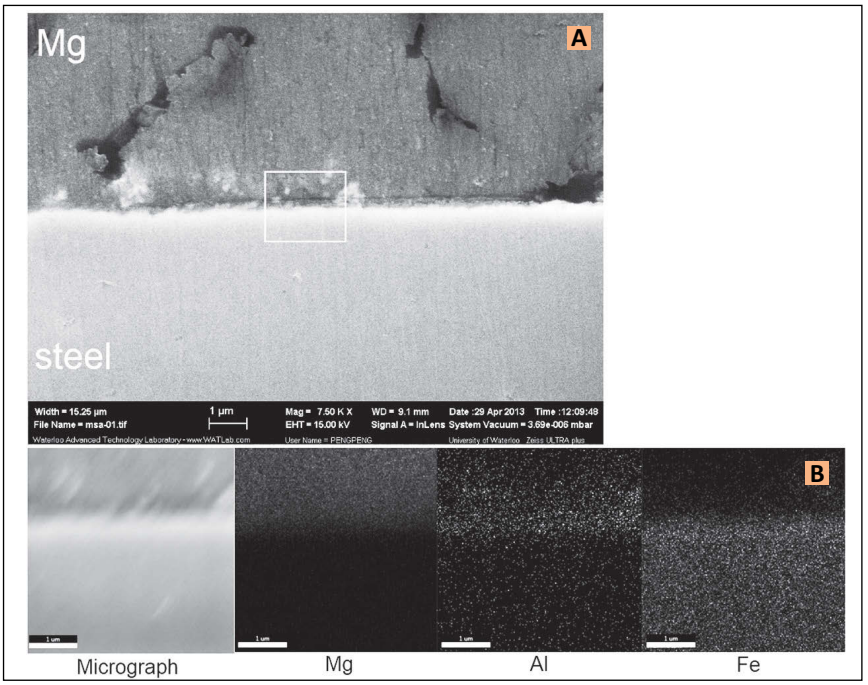

Fig. 9 — Center of Mg/steel interface of the weld made with Zn-coated steel interlayer and 28-kA welding current. A — SEM micrograph; B — element distribution map of region marked in A.

Table 3 — Energy-Dispersive X-ray Analysis Quantification of Different Areas in Fig. 8 (wt-%)

Spectrum	Al	Fe	Mg	Zn
7	53.6	46.4	—	—
8	97.4	—	2.6	—
9	67.0	30.9	2.1	—
10	42.6	57.4	—	—
11	94.8	2.8	2.4	—
12	96.8	—	3.2	—
13	36.2	—	—	63.8

Mg/Steel Interface

Interfacial Microstructure

There are three different microstructural zones in the Mg/steel interface. Similarly to the Al/steel interface, a region inside the fusion nugget was marked as MS-I, the region adjacent to the nugget as MS-II, and region beyond MS-II where welding occurred through the Zn-rich phase, as zone MS-III. Figure 9 shows details of zone MS-I in the center, similar to the Al/steel interface where no Zn was found in the microstructure, suggesting that displacement of Zn to regions adjacent to the nugget occurred. From the element distribution map (Fig. 9B), it can be seen that an ultrathin Fe-Al layer preexisting between the Zn coating and the steel before welding is still present at the interface. This observation corresponds to the findings made by Liu et al. (Ref. 17) regarding RSW of Mg to Zn-coated steel. In experiments conducted by Liu et al., the ultrathin Fe-Al layer also remained intact during welding. Those authors also found that this layer plays a crucial role in formation of the joint.

It is known that Fe and Mg are virtually immiscible; however, the pres-

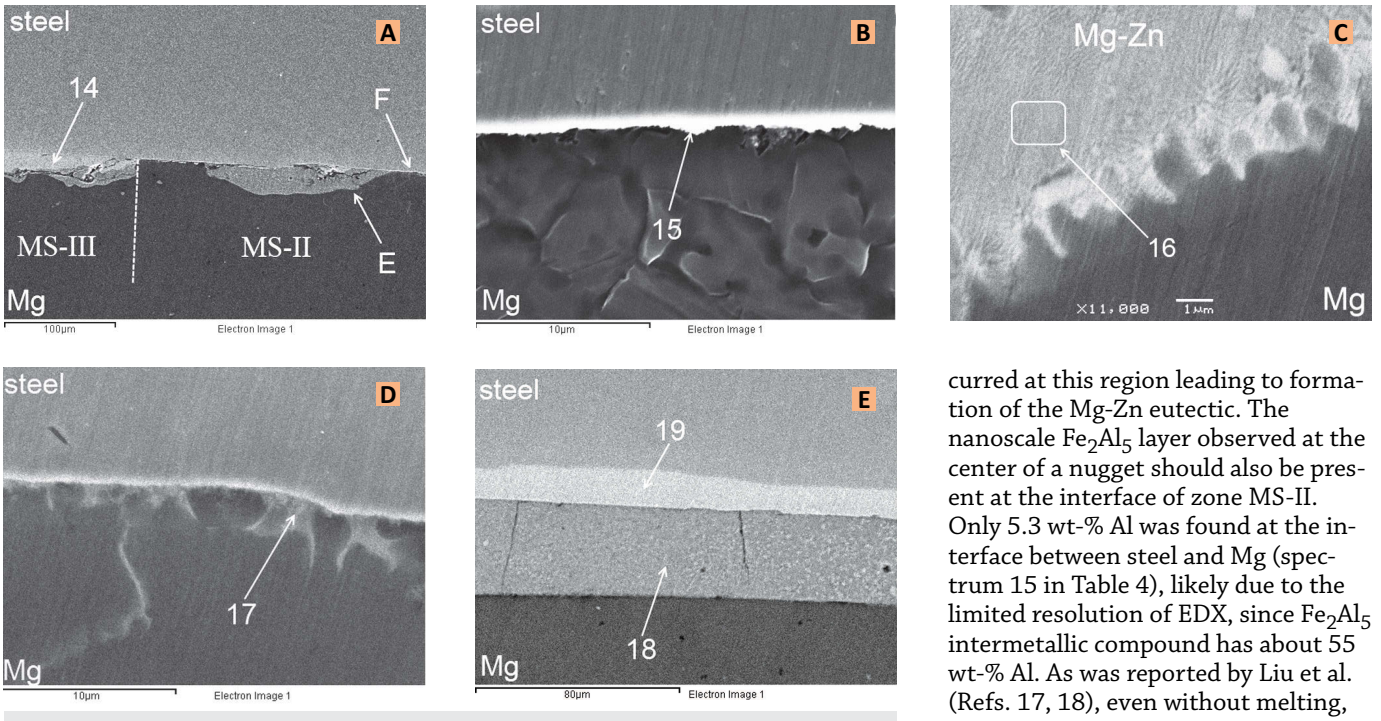

Fig. 10 — Mg/steel interface beyond the fusion zone. A — Zones MS-II and MS-III; B — zone MS-II close to the fusion nugget; C — details of E from A; D — details of F from A; E — region beyond zone MS-III.

Table 4 — Energy-Dispersive X-Ray Analysis Quantification of Different Areas in Fig. 10 (wt-%)

Spectrum	Al	Fe	Mg	Zn
14	—	—	17.3	82.7
15	5.3	52.6	42.1	—
16	—	—	45.4	54.6
17	—	8.4	65.5	26.1
18	—	—	45.2	54.8
19	—	—	—	100

ence of Al in solution at this interface may promote the formation of a high-strength joint with a nanoscale Fe_2Al_5 layer due to the edge-to-edge crystallographic planes matching (Ref. 17). Since a similar ultrathin layer of Fe_2Al_5 compound exists in all hot-dip galvanized steels (Refs. 19, 20), it can be concluded that the same welding mechanism as observed by Liu et al. took place in the current study. In addition, Tan et al. (Ref. 30) reported that during laser weld brazing of Mg to Zn-coated steel, direct contact between molten AZ31B alloy and the steel surface under the Zn coating may result in growth of the preexisting layer of Fe_2Al_5 due to diffusion of Al atoms from molten AZ31B alloy to the Fe-Al compound layer.

Figure 10 shows the Mg/steel interface at the region adjacent to the fusion nugget. None of the Zn can be found in zone MS-II close to the fusion nugget (Fig. 10B), while some accumulation of Zn-rich phase can be found at the edge of zone MS-II close to the boundary with zone MS-III, such as shown in Fig. 10A. The microstructure (Fig. 10C) and chemical composition (spectrum 16 in Table 4) of these accumulations suggest that this is a Mg-Zn eutectic with a fine lamellar structure. The Zn also was dispersed into the Mg fusion zone in regions surrounding Zn accumulations in MS-II — Fig. 10D. Despite the fact that zone MS-II located outside the fusion nugget (Fig. 5), it is possible that partial melting of the Mg sheet still occurred at this region leading to formation of the Mg-Zn eutectic. The nanoscale Fe_2Al_5 layer observed at the center of a nugget should also be present at the interface of zone MS-II. Only 5.3 wt-% Al was found at the interface between steel and Mg (spectrum 15 in Table 4), likely due to the limited resolution of EDX, since Fe_2Al_5 intermetallic compound has about 55 wt-% Al. As was reported by Liu et al. (Refs. 17, 18), even without melting, metallurgical welding between Mg and steel can occur in the region adjacent to the nugget, which is accommodated by an ultrathin Fe_2Al_5 layer.

Microstructures produced in zone MS-III can be seen in Fig. 10A. In this region, steel was bonded to Mg through the Zn-rich filler metal, which is marked as region 14 on Fig. 10A. A Zn-rich phase, which acted as a solder metal, was squeezed to zone MS-III from zones MS-I and MS-II. A similar phenomenon was observed by Liu et al. (Ref. 18) during RSW of Mg to steel, where the Zn coating was melted and completely squeezed from the nugget toward surrounding regions where it played the role of a brazing material, which contributed to overall welding area and increased fracture strength.

Figure 10E shows the Mg/steel interface beyond the MS-III zone. A significant amount of squeezed Zn phase (region 18 in Fig. 10E) and intact original Zn-coating (region 19 in Fig. 10E) can be observed in the region. The presence of a high amount of Mg in the squeezed Zn-rich phase (spectrum 18 in Table 4) suggests that Zn first reacted with Mg and then was squeezed out of the nugget. It is likely that some amount of this Zn-rich phase was not completely squeezed, which resulted in the formation of Mg-Zn eutectic in some areas in zone MS-II — Fig. 10C. The microstructure suggests that no

joining occurred in the region, since the original Zn coating remained intact.

Overall, an interfacial microstructure suggests that bonding occurred between Mg and steel in zones MS-I, MS-II, and MS-III marked on Fig. 5, while no joining occurred beyond zone MS-III. Similar to the case of the Al/steel interface, joining occurred in the Mg/steel interface by direct weld brazing in zone MS-I, by solid-state welding in zone MS-II, and brazing through Zn-rich filler metal in zone MS-III. However, much fewer voids were observed at the Mg/steel interface, which as well as the larger nugget size at Mg side likely led to the stronger joining and therefore welds failed at the Al/steel interface.

Conclusions

This study investigated mechanical and microstructural properties of Al/Mg dissimilar welds made by RSW with Zn foil and Zn-coated steel interlayers. Poor strength joints were produced with a Zn foil interlayer due to formation of brittle intermetallic phases. A Zn-coated steel interlayer was utilized to prevent mixing of the Al and Mg alloys, resulting in much higher strength of the welds. Failure load reached 74% of the same size similar AZ31B joints. The welds made with welding currents of 28 kA and higher met the strength requirements of the AWS D17.2 standard. Similar joining mechanisms took place at the Al/steel and Mg/steel interfaces. The joint area on both Al and Mg sides can be divided into three regions from the center to the edge: weld brazing of molten metal, solid-state welding, and soldering of Al (or Mg) to steel via the Zn-rich filler metal. In the fusion nugget area, Al was joined to steel by formation of a continuous Fe-Al intermetallic compound layer with a maximum thickness of 1.3 μm. Mg was joined to steel mainly through the ultrathin Fe-Al intermetallic layer that was prefabricated on the steel surface during the galvanizing process.

References

1. Borrisutthekul, R., Miyashita, Y., and Mutoh, Y. 2005. Dissimilar material laser welding between magnesium Alloy AZ31B and aluminum Alloy A5052-O. *Science and Technology of Advanced Materials* 6(2): 199–204.

2. Liu, P., Li, Y., Geng, H., and Wang, J. 2007. Microstructure characteristics in TIG welded joint of Mg/Al dissimilar materials. *Materials Letters* 61(6): 1288–1291.

3. Liu, L., and Wang, H. 2011. Microstructure and properties analysis of laser welding and laser weld bonding Mg to Al joints. *Metallurgical and Materials Transactions* A 42(4): 1044–1050.

4. Zhang, H., and Song, J. 2011. Microstructural evolution of aluminum/magnesium lap joints welded using MIG process with zinc foil as an interlayer. *Materials Letters* 65(21): 3292–3294.

5. Scherm, F., Bezold, J., and Glatzel, U. 2012. Laser welding of Mg Alloy MgAl3Zn1 (AZ31) to Al Alloy AlMg3 (AA5754) using ZnAl filler material. *Science and Technology of Welding & Joining* 17(5): 364–367.

6. Liu, L., Zhao, L., and Xu, R. 2009. Effect of interlayer composition on the microstructure and strength of diffusion bonded Mg/Al joint. *Materials & Design* 30(10): 4548–4551.

7. Zhao, L., and Zhang, Z. 2008. Effect of Zn alloy interlayer on interface microstructure and strength of diffusion-bonded Mg-Al joints. *Scripta Materialia* 58(4): 283–286.

8. Liu, L., Zhao, L., and Wu, Z. 2011. Influence of holding time on microstructure and shear strength of Mg-Al alloys joint diffusion bonded with Zn-5Al interlayer. *Materials Science and Technology* 27(9): 1372–1376.

9. Chang, W., Rajesh, S., Chun, C., and Kim, H. 2011. Microstructure and mechanical properties of hybrid laser-friction stir welding between AA6061-T6 Al alloy and AZ31 Mg alloy. *Journal of Materials Science & Technology* 27(3): 199–204.

10. Zhang, J., Luo, G., Wang, Y., Shen, Q., and Zhang, L. 2012. An investigation on diffusion bonding of aluminum and magnesium using a Ni interlayer. *Materials Letters* 83: 189–191.

11. Liu, L., Liu, X., and Liu, S. 2006. Microstructure of laser-TIG hybrid welds of dissimilar Mg alloy and Al alloy with Ce as interlayer. *Scripta Materialia* 55(4): 383–386.

12. Gao, M., Mei, S., Li, X., and Zeng, X. 2012. Characterization and formation mechanism of laser welded Mg and Al alloys using Ti interlayer. *Scripta Materialia* 67: 193–196.

13. Patel, V., Bhole, S., and Chen, D. 2012. Improving weld strength of magnesium to aluminium dissimilar joints via tin interlayer during ultrasonic spot welding. *Science and Technology of Welding & Joining* 17(5): 342–347.

14. Wang, Y., Luo, G., Zhang, J., Shen, Q., and Zhang, L. 2013. Microstructure and mechanical properties of diffusion-bonded Mg-Al joints using silver film as interlayer. Materials Science and Engineering: A 559: 868–874.

15. Shang, J., Wang, K., Zhou, Q., Zhang, D., Huang, J., and Li, G. 2012. Microstructure characteristics and mechanical properties of cold metal transfer welding Mg/Al dissimilar metals. *Materials & Design* 34: 559–565.

16. Penner, P., Liu, L., Gerlich, A., and Zhou, Y. 2013. Feasibility study of resistance spot welding of dissimilar Al/Mg combinations with Ni based interlayers. *Science and Technology of Welding & Joining* 18(7): 541–550.

17. Liu, L., Xiao, L., Feng, J., Li, L., Esmaeili, S., and Zhou, Y. 2011. Bonding of immiscible Mg and Fe via a nanoscale Fe_2Al_5 transition layer. *Scripta Materialia* 65(11): 982–985.

18. Liu, L., Xiao, L., Feng, J., Tian, Y., Zhou, S., and Zhou, Y. 2010 The mechanisms of resistance spot welding of magnesium to steel. *Metallurgical and Materials Transactions* A 41(10): 2651–2661.

19. Culcasi, J., Sere, P., Elsner, C., and Sarli, D. 1999. Control of the growth of zinc–iron phases in the hot-dip galvanizing process. *Surface and Coatings Technology* 122(1): 21–23.

20. Lee, H., and Kim, J. 2001. Effect of Ni addition in zinc bath on formation of inhibition layer during galvannealing of hot-dip galvanized sheet steels. *Journal of Materials Science Letters* 20(10): 955–957.

21. Qiu, R., Shi, H., Zhang, K., Tu,Y., Iwamoto, C., and Satonaka, S. 2010. Interfacial characterization of joint between mild steel and aluminum alloy welded by resistance spot welding. *Materials Characterization* 61(7): 684–688.

22. Qiu, R., Iwamoto, C., and Satonaka, S. 2009. Interfacial microstructure and strength of steel/aluminum alloy joints welded by resistance spot welding with cover plate. *Journal of Materials Processing Technology* 209(8): 4186–4193.

23. Qiu, R., Iwamoto, C., and Satonaka, S. 2009. The influence of reaction layer on the strength of aluminum/steel joint welded by resistance spot welding. *Materials Characterization* 60(2): 156–159.

24. *ASM Handbook*, Vol. 2 — Properties and selection: Nonferrous alloys and special-purpose materials. 1990. Materials Park, Ohio: ASM International.

25. Aalco, Aluminium Alloys — Aluminium 5754 Properties, Fabrication and Applications, Supplier Data by Aalco, 2011 [viewed January 16, 2014]. Available from *www.azom.com/article.aspx?ArticleID=2806*.

26. Penner, P. 2013. Resistance spot welding of Al to Mg with different interlayers. M.Sc. thesis. Waterloo, Ont., University of Waterloo.

27. Liu, L., Zhou, S., Tian, Y., Feng, J., Jung, J., and Zhou, Y. 2009. Effects of surface conditions on resistance spot welding of Mg alloy AZ31. *Science and Technology of Welding & Joining* 14(4): 356–361.

28. Liu, L., Xiao, L., Feng, J., Tian, Y., Zhou, S., and Zhou, Y. 2010. Resistance spot welded AZ31 magnesium alloys, Part II: Effects of welding current on microstructure and mechanical properties. *Metallurgical and Materials Transactions A* 41(10): 2642–2650.

29. Tan, W., Zhou, Y., and Kerr, H. 2002. Effects of Au plating on small-scale resistance spot welding of thin-sheet nickel. *Metallurgical and Materials Transactions A* 33(8): 2667—2676.

30. Tan, C., Li, L., Chen, Y., Mei, C., and Guo, W. 2013. Interfacial microstructure and fracture behavior of laser welded-brazed Mg alloys to Zn-coated steel. *The International Journal of Advanced Manufacturing Technology* DOI10.1007/s00170-013-4910-4.